

# Chapter 2

## Modulo-Type Precoding for Networks

Robert F.H. Fischer, Michael Cyran, Sebastian Stern  
and Johannes B. Huber

**Abstract** In this chapter, we address scenarios where the tasks of (modulo-type) precoding for the multiple-input/multiple-output (MIMO) broadcast channel, network coding with its associated finite-field matrix channel, and channel coding meet or complement each other. By enlightening dualities, similarities, and differences between the areas and corresponding schemes, a deeper understanding of their mutual interaction is gained. Moreover, this allows for a transfer of schemes and strategies from one field to another one. Exemplarily, schemes operating at the intersection of complex-valued and finite-field/modulo processing are addressed. First, an overview on modulo-type precoding and its latest version via finite-field preprocessing is given; the connections and specific restrictions of the different approaches are illustrated. The advantages of modulo-type precoding are addressed when additional requirements, such as per-antenna power constraints and a reduced degree of coordination in a network MIMO scenario, are imposed. Finally, the application of precoding to finite-field channels is discussed, either as differential network coding or as selection precoding.

### 2.1 Introduction

Since two decades, the interest in communication schemes with multiple input and multiple output signals, forming a so-called *multiple-input/multiple-output (MIMO) channel*, has grown enormously. Meanwhile, MIMO techniques are in the standard

---

R.F.H. Fischer (✉) · S. Stern  
Ulm University, Albert-Einstein-Allee 43, 89081 Ulm, Germany  
e-mail: robert.fischer@uni-ulm.de

S. Stern  
e-mail: sebastian.stern@uni-ulm.de

M. Cyran · J.B. Huber  
FAU Erlangen-Nürnberg, Cauerstrasse 7, 91058 Erlangen, Germany  
e-mail: michael.cyran@fau.de

J.B. Huber  
e-mail: johannes.huber@fau.de

repertoire of each communication engineer. Not only *multi-antenna* point-to-point systems can be treated under this umbrella term, but the joint consideration of signals is particularly useful in *multi-user schemes*. Via joint processing, interference between users can be dealt with in a constructive way, rather than as unavoidable, noise-like disturbance.

Interference and joint processing can occur/be performed on different layers in the OSI communication model. In this chapter, we address the *physical* and the *network* layer. Specifically, *modulo-type precoding* [19] and *network coding* [15] are considered, which have been subject of immense research activity over the last decade. Even though these techniques pursue similar or dual purposes, up to now interdependencies between the areas have only rarely been investigated or even utilized. In this chapter, we address scenarios where the tasks of (modulo-type) precoding, network coding, and channel coding meet or complement each other. By enlightening dualities, similarities, and differences between the fields and corresponding schemes, a deeper understanding of their mutual interaction is gained. Moreover, this allows for a transfer of schemes and strategies from one field to another one.

First, we present the broadcast channel and the finite-field matrix channel which arises in network coding. Then, similarities and dualities are briefly discussed. In Sect. 2.2, the connection between complex-valued and finite-field channels is depicted for the situation of precoding for the broadcast channel. Even though the channel is real-/complex-valued, the use of finite-field arithmetic for precoding is an interesting new option. The optimization of wireless multi-base-station schemes w.r.t. per-antenna power constraints is considered in Sect. 2.3. The possibility of reducing the required (wired) backhaul traffic employing a decentralized processing with hierarchical coordination among base stations and via finite-field precoding are given. Finally, in Sect. 2.4, precoding is applied to finite-field channels. Differential linear network coding and selection precoding are techniques transferring knowledge from the continuous to the finite-field world, thereby enabling new degrees of freedom in system design.

### 2.1.1 MIMO Broadcast Channel

A block diagram of the MIMO *broadcast channel (BC)*, describing the downlink transmission from a central *base station (BS)*, equipped with  $B$  antennas, to  $K$  independent, non-cooperating *user equipments (UEs)* is visualized in Fig. 2.1. The fundamental input/output relation is given by

$$\mathbf{y} = \mathbf{H}\mathbf{x} + \mathbf{n} , \quad (2.1)$$

where  $\mathbf{x} = [x_1, \dots, x_B]^T \in \mathbb{C}^B$  is the vector of transmit symbols,  $\mathbf{y} = [y_1, \dots, y_K]^T \in \mathbb{C}^K$  the vector of receive symbols,  $\mathbf{n} = [n_1, \dots, n_K]^T \in \mathbb{C}^K$  is the noise vector and

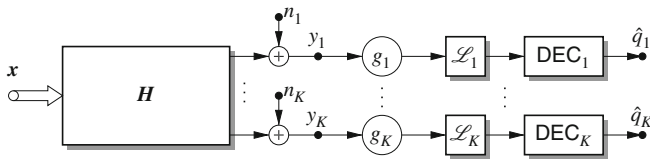


**Fig. 2.1** Broadcast channel, i.e., downlink transmission from a central base station with  $B$  antennas (joint transmit vector  $\mathbf{x}$ ) to the  $K$  individual users (scaling  $g_k$ , metric calculation  $\mathcal{L}_k$ , and channel decoding)

$$\mathbf{H} = [h_{k,b}]_{\substack{k=1,\dots,K \\ b=1,\dots,B}} \quad (2.2)$$

is the  $K \times B$  channel matrix collecting the channel gains  $h_{k,b}$  when assuming flat fading channels.<sup>1</sup> We stick to the standard assumption of a *block-fading channel*, i.e., it is randomly drawn according to some (known) distribution, but remains constant over a transmission burst. The transmit symbols are expected to be zero-mean and with variance  $\sigma_x^2 \stackrel{\text{def}}{=} \mathbb{E}\{|x_b|^2\}$ ,  $b = 1, \dots, B$ , and the zero-mean white Gaussian noise has variance  $\sigma_n^2 \stackrel{\text{def}}{=} \mathbb{E}\{|n_k|^2\}$ ,  $k = 1, \dots, K$ . Please note, since the channel is modeled in the *equivalent complex baseband*, all signals and coefficients are complex-valued. Unless otherwise stated, we assume perfect channel knowledge at the joint transmitter.

### 2.1.2 Finite-Field Matrix Channels

Meanwhile, *finite-field matrix channels*—i.e., MIMO channels where all quantities are drawn from and the arithmetic is carried out over a finite field—emerged in several situations, in particular in (*random*) *linear network coding* ((*R*)*LNC*) [40] or in lattice-coded MIMO systems, where *integer-forcing* (*IF*) [25, 33] receivers or transmitters are employed (cf. also Sect. 2.2.3). The most general form is the *multiplicative additive matrix channel* (*MAMC*) [40], depicted in Fig. 2.2. Its input-output relation reads

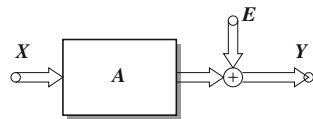
$$\mathbf{Y} = \mathbf{A}\mathbf{X} + \mathbf{E}. \quad (2.3)$$

Here, usually *packets* (or codewords, vectors) of length  $l$  (equivalent to  $l$  time steps in the BC) are considered and  $n$  packets are fed to the network in parallel.<sup>2</sup> Thus, the transmit signal is given as matrix  $\mathbf{X} \in \mathbb{F}_q^{n \times l}$ . The linear channel, modeled by the channel matrix  $\mathbf{A} \in \mathbb{F}_q^{N \times n}$ , multiplicatively distorts  $\mathbf{X}$  and superimposes an additive

<sup>1</sup>If, in addition to the multi-user interference, intersymbol interference (ISI) occurs, the usual way is to apply orthogonal frequency-division multiplexing (OFDM) to deal with the ISI. The MIMO model is then valid per subcarrier.

<sup>2</sup>In terms of RLNC, one channel usage, i.e., the transmission of one transmit and the reception of one receive matrix, is called one *generation*. In terms of the BC, this is a transmission burst.

**Fig. 2.2** Multiplicative additive matrix channel



error, expressed by an error matrix  $E \in \mathbb{F}_q^{N \times l}$ . The quantities  $n$  and  $N$ , with  $N \geq n$ , denote the numbers of transmit and receive packets, respectively. In RLNC,  $A$  is randomly chosen (typically uniformly over all full-column-rank  $(N \times n)$  matrices over  $\mathbb{F}_q$  [9] and may change after each packet [40].

For some applications it is reasonable to consider two types of degenerated finite-field matrix channels, namely the *multiplicative matrix channel* (MMC)  $Y = AX$ , and the *additive matrix channel* (AMC)  $Y = X + E$ .

### 2.1.3 Analogies and Dualities

In communications and information theory, analogies and dualities are very helpful and powerful tools. A famous example is the duality between *source coding* and *channel coding* [17, 24]. In source coding redundancy is eliminated, while in channel coding redundancy is deliberately added. Via this duality, schemes from the one field can be converted to the other one, cf. [16, 58].

Another prominent example is the *uplink/downlink duality* [28, 38, 46, 47, 56], which states that the *multiple-access channel* and the *broadcast channel* are dual to each other. This not only led to the derivation of the capacity region of the BC [49] but also sparked the design of transmitter-side techniques which are dual to receiver-side approaches, cf. *Tomlinson-Harashima precoding (THP)* as the dual to *decision-feedback equalization (DFE)* (aka successive interference cancellation [20]), or *vector precoding* [35] as the dual to *maximum-likelihood detection*.

Besides such dualities, *analogies* and *similarities* are of major importance. As can be seen from Figs. 2.1 and 2.2 or (2.1) and (2.3), respectively, the MIMO BC and the MAMC are counterparts to each other, existing in two different worlds of arithmetics. Moreover, *precoding (PC)* for the MIMO BC (see Sect. 2.2) and *network coding (NC)* share some general principles, too. In both fields a number of incoming signals are treated jointly, as can be seen in Fig. 2.3. *Modulo-linear combinations* of the signals  $X_a$  and  $X_b$  (in NC) and of the signal  $a$  and the interference  $f$  (in PC), respectively, are calculated and processed. However, due to the different fields  $\mathbb{F}_q$  and  $\mathbb{C}$  the modulo operation is inherent (and given) in the one situation but has to be forced (and can be designed [1]) in the other one. Moreover, the important parameter of (transmit) power, obvious over  $\mathbb{C}$ , is not existent over  $\mathbb{F}_q$  or has to be defined explicitly as a cost (cf. Sect. 2.4).

In the following sections, we exemplarily address schemes operating at the intersection of complex-valued and finite-field/modulo processing. First, an overview on modulo-type precoding and a recent proposal using finite-field preprocessing is

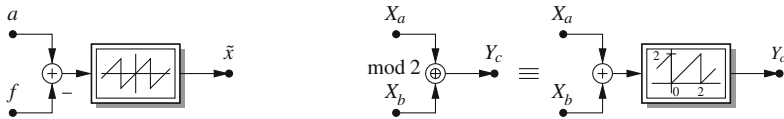


**Fig. 2.3** General principles of precoding for the BC (*left*) and (binary) network coding (*right*)

given; the connections and differences of the approaches are illustrated. The advantage of precoding when additional constraints are imposed is addressed. Finally, the application of precoding to finite-field channels is discussed.

## 2.2 Connection Between Complex-Valued and Finite-Field Channels in Precoding

Precoding for the broadcast channel has now been studied since more than one decade and has undergone significant developments. Still, one of the fundamental bases for the treatment of this scenario is the *uplink-downlink duality* [38, 46, 47, 56]. As a result, schemes developed for the joint reception in a multipoint-to-point scenario are transferred (dualized) to joint transmitter-side processing. However, very recently, a new concept entered the scene: the connection between complex-valued and finite-field calculations. In this section, we briefly review the different variants of preprocessing for the broadcast channel and highlight the respective advantages. In particular, we discuss the combination of channel coding with the respective precoding scheme.

### 2.2.1 Conventional Schemes

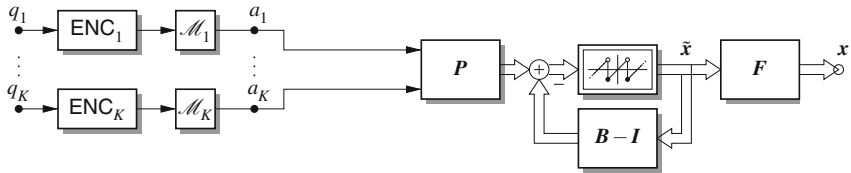
The simplest version of precoding for the broadcast channel is *linear preequalization (LPE)*, cf. Fig. 2.4, first row. If the preprocessing matrix  $\mathbf{W}$  is chosen according to the *zero-forcing (ZF)* criterion, it is simply the (right pseudo) inverse of the channel matrix  $\mathbf{H}$ . In MIMO communications, significant gains can be achieved optimizing the processing according to the *minimum mean-squared error (MMSE)* criterion, trading off transmit power enhancement (the dual to noise enhancement in receiver-side equalization) and residual interference. Since decoupled AWGN channels for the users are created, each user can employ any conventional channel coding scheme ( $\text{ENC}_k$ ) and mapping to signal points ( $\mathcal{M}_k$ ) known from the AWGN channel.

Some improvements can be obtained if *Tomlinson-Harashima Precoding (THP)* is used, see Fig. 2.4, second row. The main idea is to employ *modulo arithmetics* which can be interpreted as representing data by a multiplicity of signal points and selecting the most suited one in a symbol-by-symbol fashion [19]. Via the feedforward matrix

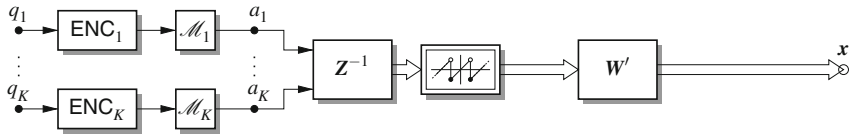
## Linear Preequalization



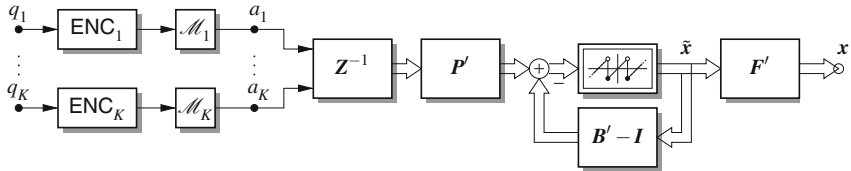
## Tomlinson-Harashima Precoding



## Lattice-Reduction-Aided Linear Preequalization



## Lattice-Reduction-Aided Precoding



## Integer-Forcing Preequalization

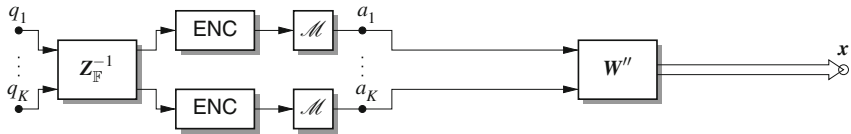


**Fig. 2.4** Visualization of the various precoding concepts for the broadcast channel. *Top to bottom* linear preequalization; Tomlinson-Harashima precoding; lattice-reduction-aided linear preequalization; lattice-reduction-aided precoding; integer-forcing (linear) preequalization

$\mathbf{F}$ , the channel matrix is transformed to lower triangular (spatially causal) form. The transmit symbols are generated successively via the feedback loop (lower triangular, unit main diagonal feedback matrix  $\mathbf{B}$ ); the modulo device restricts the amplitude and hence the transmit power. The optimization of the encoding order is described by the permutation matrix  $\mathbf{P}$ . Noteworthy, as in LPE, channel coding can be employed on top of the equalization scheme. However, due to the inherent modulo congruence, the set partition in the coded modulation scheme has to match with the multiple

representation, i.e., the partitions also have to be modulo periodic and the receiver-side decoding (metric calculation  $\mathcal{L}_k$  and  $\text{DEC}_k$  in Fig. 2.1) has to take the periodic extension into account [19].

Using uncoded transmission, both schemes, LPE and THP (regardless whether optimized according to the ZF or MMSE criterion), exhibit only a diversity order of one.

### 2.2.2 Lattice-Reduction-Aided Schemes

In 2002/03 the concept of *lattice-reduction-aided (LRA)* equalization has been introduced in [55] and then generalized and transferred to precoding in [41, 51, 52]. The main idea is, not to equalize the channel itself, but to find a more suited description.

When using signal constellations drawn from a regular grid, the signal points at the output of a MIMO channel form (a subset of) a *lattice*. However, each lattice can be described by different bases—for equalization basis vectors as short and as close to orthogonality as possible are highly preferable. The task of finding such a basis is known as *lattice (basis) reduction*. Efficient algorithms for decomposing a matrix  $\mathbf{H}$  (whose rows span the lattice) according to  $\mathbf{H} = \mathbf{Z} \cdot \mathbf{H}_{\text{red}}$  exist [3, 32, 54], where  $\mathbf{Z}$  is a change-of-basis matrix with integer entries and a unit-magnitude determinant—a so-called *unimodular* matrix—and  $\mathbf{H}_{\text{red}}$  has desired properties (basically,  $\mathbf{H}_{\text{red}}^{-1}$  should cause least noise enhancement). Applying this representation in receiver-side equalization, not the transmitted signal constellation is equalized but “only” the *signal grid*. In other words, integer linear combinations of the signal points are detected. These linear combinations are, in a final step, resolved by the inverse change-of-basis matrix, which is unimodular, too.

Utilizing the uplink-downlink duality, *LRA linear preequalization* and *LRA precoding* result, cf. third and fourth row in Fig. 2.4. Integer linear combinations of the (encoded and mapped) data symbols are calculated (unimodular matrix  $\mathbf{Z}^{-1}$ ) followed by either linear preequalization or THP of the so-called *reduced channel* given by  $\mathbf{H}_{\text{red}} = \mathbf{Z}^{-1} \cdot \mathbf{H}$ . It has been shown that LRA equalization/precoding achieves the full diversity order offered by the MIMO channel [44]. Noteworthy, as in the case of conventional schemes, LRA schemes can be optimized according to the ZF or the MMSE criterion, see, e.g., [4, 5, 7, 53].

It is true that LRA equalization so far has been studied almost exclusively for uncoded transmission. This is because channel coding can easily be applied independently of/cascaded with the equalization part. The only restriction, as already present in THP, is that the coded modulation fits to the periodic extension/modulo reduction. Since all data streams are encoded and decoded individually (from  $a_k$  to  $y_k, k = 1, \dots, K$ , basically independent parallel AWGN channels with periodic continuation of the signal constellation are present) each user may employ an individual code.

### 2.2.3 Integer-Forcing Schemes

Very recently, a new philosophy for equalization in MIMO schemes, named *integer forcing* (IF), has been proposed [59]. It originates from *compute-and-forward* relaying schemes [33] and physical-layer network coding [18] and is closely related to LRA equalization with subtle, however essential differences. A precoding version of the integer-forcing strategy for distributed antenna systems, termed *reverse compute-and-forward* (RCoF), has been presented in [25].

The main difference, when comparing the third (LRA LPE) and last (IF) row in Fig. 2.4, is that the order of channel encoding and equalization of the integer part is reversed. Not the encoded symbols are linearly combined but the information symbols prior to encoding. In doing so, it has to be assumed that in IF the source symbols are drawn from the finite field  $\mathbb{F}_p$ , where  $p$  is a prime. In our view, the restriction to a prime field is the much more important conceptional difference between LRA and IF than that of studying uncoded and coded transmission, respectively; we cannot share the view given in [59, Bottom of Page 7678]. Indeed, considering uncoded transmission, a signal constellation whose cardinality  $M$  is a prime, and employing a so-called linear mapping [18] (in its simplest case the natural mapping of the finite-field elements  $0, 1, \dots, p-1$  to the integers  $0, 1, \dots, p-1$ ), both versions are identical.

In LRA equalization integer linear combinations of data symbols/code words in the signal space are decoded. In order to resolve these linear combinations by calculating only integer combinations (over  $\mathbb{R}$ ), the integer matrix (change-of-basis matrix)  $\mathbf{Z}$  has to be unimodular (see above). In IF this resolving is done over the finite field—an inverse matrix has to exist over  $\mathbb{F}_p$ , only. In turn, the finite-field equivalent to the integer matrix,  $\mathbf{Z}_{\mathbb{F}}$ , may have any determinant.

A comparison of the respective rows in Fig. 2.4 reveals that in LRA and IF modulo- $M$  integer linear combinations are calculated prior to the linear equalization of the residual (reduced) part of the channel. First, the modulo reduction (equivalence modulo  $M$ ) relaxes the constraints on the existence of  $\mathbf{Z}^{-1}$ ; not an inverse over  $\mathbb{R}$  is required but only over  $\mathbb{Z}_M$ , the integers modulo  $M$ . If  $M = p$  is a prime we have  $\det(\mathbf{Z}) \in \mathbb{Z} \setminus M\mathbb{Z}$ ; in this case (and assuming linear encoding) the operations in LRA and IF, respectively, are completely equivalent as the arithmetic of the prime field  $\mathbb{F}_p$  is identical to that of calculating over  $\mathbb{Z} \bmod p$ . Second, having a close look at the operation of LRA LPE, it is revealed that  $\mathbf{Z}$  may have any determinant unequal to zero. Performing all operations over the integers preserves the discrete nature of the signal constellation; inverting a non-unit determinant matrix  $\mathbf{Z}$  over the reals destroys the regular structure of the symbols prior to  $\mathbf{W}'$  but precoding still works. Third, it can be shown that IF even works for the more practical case of  $M$  not being a prime, in particular  $M = 2^m$ ,  $m \in \mathbb{N}$ . Here,  $\det(\mathbf{Z}) \in 2\mathbb{Z} + 1$  is required. Numerical simulations do not show a clear advantage for one of the strategies.

Noteworthy, by replacing the preequalization matrix  $\mathbf{W}''$  with a THP structure, an integer-forcing precoding strategy would be possible as well (not shown here; cf. also the receiver-side counterpart [34]).



Dropping the unimodular constraint on  $\mathbf{Z}$  in the IF strategy has two main disadvantages. First, up to now, no well-performing and efficient strategy on calculating  $\mathbf{Z}$  with arbitrary determinant is available; see the “full” search in [59], the distributed approach in [25], or again the lattice-reduction strategy in [37]. Despite channel matrices can be constructed where IF provides an infinite gain over LRA equalization (cf. [59, Appendix A]), no gains for i.i.d. Rayleigh fading channels could be observed up to now. Second, IF precoding requires the employment of identical channel codes for the users; in case of different desired rates, the lower-rate codes have to be subcodes of the highest-rate code [25]. This gives less flexibility in the system design than in an LRA scheme. However, in distributed antenna systems (coordinated multipoint, network MIMO, see also Sect. 2.3) IF is of interest. If, as in [25], the residual equalization via  $\mathbf{W}'' \approx \mathbf{H}_{\text{red}}^{-1}$  is not present, only finite-field symbols have to be communicated from the central unit over the backhaul network to the base stations, which perform the encoding of the precombined source words.

To conclude, the IF philosophy has changed the perspective on LRA schemes and has sparked new research eliminating the unnecessary restrictions imposed up to now. However, as LRA schemes are already diversity-optimum, no further immense gains can be expected.

## 2.2.4 Summary

As a summary, Table 2.1 compares the discussed precoding schemes w.r.t. the equalization task, the utilized degree of freedom, and the constraints on the signal constellations and the codes.

**Table 2.1** Comparison of linear preequalization (LPE), Tomlinson-Harashima precoding (THP), LRA preequalization/precoding (LRA), and integer-forcing preequalization (IF) w.r.t. the equalization task, the utilized degree of freedom, and the constraints on the signal constellations and the codes

	Equalization task (ZF case)	Degree of freedom	Constraints on signal constellation	Constraints on codes
LPE	$\mathbf{H}\mathbf{W} = \mathbf{I}$ full equal	–	–	Codes for AWGN channel can be used
THP	$\mathbf{P}\mathbf{H}\mathbf{F} = \mathbf{B}$ Lower triangular	Modulo-congruent signal points	Periodic continuation required	Have to work under modulo reduction
LRA	$\mathbf{H}\mathbf{W}' = \mathbf{Z}$ Integer unimodular matrix	Integer linear combinations	Integer lin. comb. and periodic continuation required	Have to work under modulo reduction
IF	$\mathbf{H}\mathbf{W}'' = \mathbf{Z}$ Integer matrix	Integer linear combinations	Integer lin. comb. and periodic continuation required	Same code for UEs; Has to work under modulo reduction

### 2.3 Precoding for Distributed MIMO

In *distributed MIMO* (also denoted as *network MIMO* or *coordinated multipoint*), e.g., [29], a number of non-located *base stations* (BSs) are grouped and jointly communicate with a number of (non-cooperating) *user equipments* (UEs), distributed over some service area. Assuming perfect coordination of the BSs, a variant of the BC is present and hence all preequalization/precoding strategies (cf. Fig. 2.4) for the MIMO broadcast channel can be employed.

However, since the transmit antennas are not at the same location some important extra considerations have to be taken into account. First, in addition to the usual *sum power constraint* (SPC), here a *per-antenna power constraint* (APC) is of much more interest; this problem is addressed in Sect. 2.3.1. Second, since the data has to be communicated to/between the BSs, the coordination effort and the respectively induced backhaul traffic has to be taken into account; see Sects. 2.3.2 and 2.3.3.

The most obvious network MIMO downlink scenario, used, e.g., in [6, 11, 12, 42], is illustrated in the left part of Fig. 2.5 (denomination of the symbols as in Fig. 2.4). In our example,  $B = 3$  BSs (with sectorized antennas and taken from a larger arrangement of BSs; distance  $r_{BS}$ ) serve the shaded area, where  $K = 3$  single-antenna UEs are located. Since network MIMO is particularly suited for supplying cell-edge regions, UEs close to BSs (distance smaller than  $r_{min}$ ) may be excluded from joint processing, cf. [6, 11]. The channel matrix  $\mathbf{H}$  for this scenario can be derived from the geometry and includes the antenna pattern, attenuation, path loss, and shadowing as well as fast fading effects. Details can be found in [6, 13, 14, 42].

In network MIMO, the BSs are usually connected to a central unit (CU) via wired backhaul links enabling the coordinated transmission.

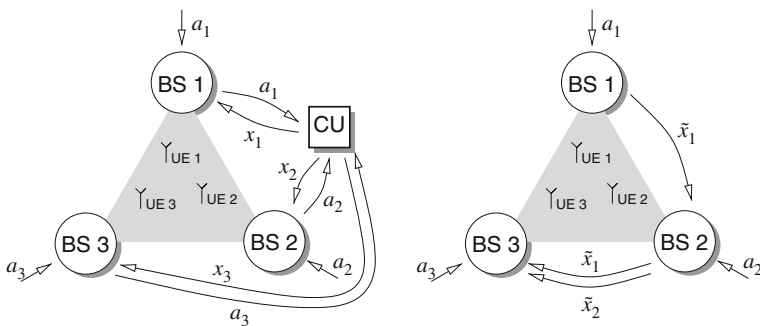


**Fig. 2.5** Geometrical network MIMO system model for  $B = 3$  and  $K = 3$ . *Left* full coordination via a central unit (CU); *Right* hierarchical scheme without central instances

### 2.3.1 Optimization Under Per-Antenna Power Constraints

In the literature, the optimization of LPE subject to a per-antenna power constraint has been given in [45, 57]. Recently, such an additional constraint has been applied to the more advanced precoding versions, cf. [6].

The performance is preferably expressed in terms of the *signal-to-interference-plus-noise ratio* (SINR) of the users. Let the users be renumbered according an optimized processing order (obtained, e.g., from conventional THP and described by a permutation matrix  $\mathbf{P}$ ). Then, the SINR of user  $u$  in case of THP, cf. Fig. 2.4, second row, is given by

$$\text{SINR}_k \stackrel{\text{def}}{=} \frac{|c_{k,k}|^2}{\frac{\sigma_n^2}{\sigma_a^2} + \sum_{l, l>k} |c_{k,l}|^2}, \quad (2.4)$$

where  $\mathbf{C} = [c_{k,l}] = \mathbf{H}\mathbf{F}$  denotes the *end-to-end cascade* from data to receive symbols. Due to successive encoding in THP, users with lower index (processed first) do not contribute to the interference. This main advantage over linear schemes can be used to “shape” the interference [6].

Knowing the actual channel realization, it is appropriate to adjust the precoding scheme such that the minimum SINR over all users is maximized. Hence, the optimization task (minSINR criterion) for finding the optimum feedforward matrix  $\mathbf{F}$  reads

$$\arg\max_{\mathbf{F}} \min\text{SINR} \stackrel{\text{def}}{=} \arg\max_{\mathbf{F}} \min_{k=1,\dots,K} \text{SINR}_k, \quad (2.5)$$

taking the SPC  $\mathbb{E}\{\mathbf{x}^H\mathbf{x}\} \leq P_{\text{sum}}$  and the APC  $\mathbb{E}\{|x_b|^2\} \leq P_{\text{per}}, b = 1, \dots, B$ , into account. After the determination of the feedforward matrix  $\mathbf{F}$ , the gain matrix  $\mathbf{G} = \text{diag}(g_1, \dots, g_K)$ , cf. Fig. 2.1, is adjusted such that  $\mathbf{G}\mathbf{H}\mathbf{F}$  has unit main diagonal, and the feedback matrix  $\mathbf{B}$  is given as the lower triangular part thereof.

This resulting optimization task may be solved by resorting to a *second-order cone program*, cf. [45, Algorithm 2]. The sorting according to the *BLAST algorithm* [21, 23] almost always provides the optimum ordering (permutation matrix  $\mathbf{P}$ ) [50].

Figure 2.6 shows the bit error rate (BER) curves<sup>3</sup> assuming uncoded transmission (16-ary QAM constellation with Gray labeling and variance  $\sigma_a^2$ ) for the  $K \times B = 3 \times 3$  network MIMO system model. The channel parameters are taken from [6, 13, 14]. Either no (gray curves) or a per-antenna power constraint of  $P_{\text{per}} = 1.5 \sigma_a^2$  (black curves) is imposed. In each case a sum power constraint  $P_{\text{sum}} = 3 \sigma_a^2$  is active. LPE and THP are optimized according to the minSINR criterion, see also [45]. However, in case of LPE this optimization does not provide substantial gains over the conventional sum-MSE solution, where, in case of an APC, the feedforward matrix is simply scaled to meet the constraint, cf. [6].

<sup>3</sup>All results in this section are displayed over the ratio of *transmitted energy per information bit*  $E_b$  and one-sided noise power spectral density  $N'_0$ , where the average channel attenuation is eliminated. For details on the normalization, see [6].

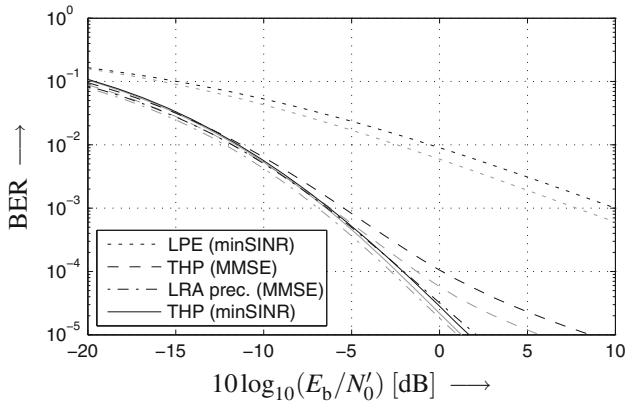


**Fig. 2.6** Bit error rate over the ratio of transmitted energy per information bit  $E_b$  and equivalent noise power spectral density  $N'_0$ . Geometrical channel model with  $r_{\min} = 125$  m. *Dotted* minSINR LPE; *Dashed* MMSE THP; *Dashed-dotted* MMSE LRA precoding. *Solid* minSINR THP. *Gray* only SPC  $P_{\text{sum}} = 3\sigma_a^2$  active; *black* additional APC  $P_{\text{per}} = 1.5\sigma_a^2$ . Inter-site distance  $r_{\text{BS}} = 500$  m

As can be seen from the figure, the APC  $P_{\text{per}} = 1.5\sigma_a^2$  causes a loss of about 2.5 dB for LPE. Performance can significantly be improved if conventional MMSE THP is employed, which provides a gain of up to 15 dB over LPE. However, the curves for THP and LPE flatten out to diversity order one. Very good performance can also be obtained using LRA precoding, where the feedforward matrix is also simply scaled to meet the APC [6]. This scheme has full diversity order 3; no flattening of the BER curves occur. In the low BER regime, THP optimized according to the minSINR criterion gives even better results as both power constraints are explicitly taken into account in the optimization. An APC of  $P_{\text{per}} = 1.5\sigma_a^2$  does almost not lead to a performance degradation.

In summary, it can be stated that compared to LPE non-linear precoding is much more attractive in the network MIMO scenario with per-antenna power constraint. The individual powers at the antennas can even be restricted down to  $P_{\text{per}} = \sigma_a^2 \dots 2\sigma_a^2$  without too much loss in performance.

### 2.3.2 Coordination Effort and Hierarchical Precoding

In network MIMO using TH-type precoding, one has to distinguish between two different coordination/joint processing tasks: (i) the precoding matrices  $\mathbf{B}$  and  $\mathbf{F}$  together with the optimum permutation  $\mathbf{P}$  have to be computed, and (ii) given the data symbols (i.e., the data vector  $\mathbf{a}$ ), the vector  $\mathbf{x}$  of transmit symbols has to be calculated.

Assuming a block-fading channel (constant channel matrix  $\mathbf{H}$  over a transmission burst), the calculation of the matrices has only to be done once per channel realization. In contrast, the calculation of  $\mathbf{x}$  has to be carried out at each time step. To this end, all data may be communicated to a CU (cf. Fig. 2.5), processed, and then transferred back to the BSs. Assuming that the symbols are initially available at the BSs, this procedure requires the transmission of six complex numbers per time step. The same amount is also required for the decentralized coordination described in [11, 12], where each BS passes its knowledge to the other BSs.

Conceptually, the main part of THP is the successive encoding (feedback structure) of the data symbols. However, due to the feedforward matrix  $\mathbf{F}$ , for the calculation of each transmit symbol  $x_b$  all precoded symbols  $\tilde{x}_k$  are required. The exchange of these symbols causes the huge backhaul traffic in decentralized coordination. Let  $\beta$  denote the number of complex symbols communicated per time step, we have  $\beta = 6$  for the example at hand.

To overcome this problem, in [11, 12] a *hierarchical* distribution of knowledge among the BSs has been proposed. The thereby required backhaul transmission is indicated in the right part of Fig. 2.5 and amounts to only  $\beta = 3$ . As can be seen, the level of knowledge on the data of the other users increases from BS to BS. Such a successive procedure is only possible if the (usually joint) feedforward processing is modified; it is easy to see that such a structure is reflected in the fact that  $\mathbf{F}$  has *lower triangular* structure.

Basically, the minSINR optimization briefly discussed above can (with slight modifications) be applied to this setting, too [11]. However, in addition to the  $K! = 6$  possible permutations of the users (as in conventional THP), here also the BSs are non-equivalent and an optimized ordering (relabeling) of them has to be done. In [11], a greedy strategy has been presented to preselect a set of suited sortings among all  $K!B! = 36$  options. The minSINR optimization is then carried out for these candidates and the sorting leading to the best performance (largest minSINR) is chosen for transmission.

In Fig. 2.7, the BER obtained by numerical simulation is shown for the mentioned hierarchical scheme. Both the results for full search (all sortings tested) and the greedy preselection (six candidates) are shown. For comparison, the results for fully-coordinated schemes are repeated from Fig. 2.6 (APC  $P_{\text{per}} = 1.5 \sigma_a^2$ ). As can be seen, employing hierarchical precoding (full search), there is only a loss of about 2.5 dB in the low BER regime ( $\text{BER} \approx 10^{-4}$ ) when compared to fully joint preprocessing via THP (minSINR criterion). However, compared to LPE, which also requires  $\beta = 6$  backhaul transmissions, hierarchical THP shows significantly better results. Hierarchical THP even outperforms fully-coordinated THP optimized according to the sum MSE when considering the very-low-BER range ( $\text{BER} < 10^{-4}$ ). The greedy preselection does not cost too much in performance but lowers the initial computation effort significantly.

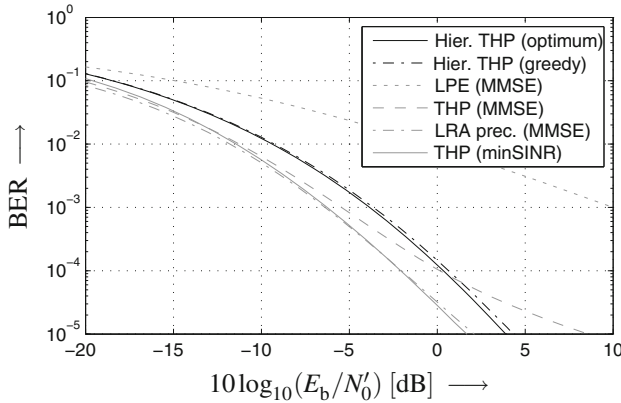


**Fig. 2.7** Bit error rate over the ratio of transmitted energy per information bit  $E_b$  and equivalent noise power spectral density  $N'_0$ . Geometrical channel model with  $r_{\min} = 125$  m. *Black solid* hierarchical THP with full search; all sortings tested. *Black dashed-dotted* hierarchical THP with greedy strategy; six candidates. *Gray curves* from Fig. 2.6 for comparison. SPC  $P_{\text{sum}} = 3 \sigma_a^2$ ; APC  $P_{\text{per}} = 1.5 \sigma_a^2$ . Inter-site distance  $r_{\text{BS}} = 500$  m

### 2.3.3 Selection of the Coordination Strategy

In many applications, a maximum tolerable BER is defined, corresponding to a minimum requirement on the SINR. If a “good” channel realization is present, the required performance may already be achieved without any precoding, hence requiring no backhaul traffic ( $\beta = 0$ ). For “medium” channel instances, hierarchical precoding is often sufficient ( $\beta = 3$ ); only in case of “bad” channel conditions, fully coordinated THP ( $\beta = 6$ ) may have to be used. In other words, the desired performance should be achieved with the smallest amount of joint processing/backhaul traffic as possible.

In [12], a selection algorithm has been proposed, which either selects hierarchical or full THP. To this end, a minimally required SINR, denoted as  $\text{minSINR}_{\text{thr}}$ , is specified, e.g., based on system requirements or on the statistical distribution of  $\text{minSINR}$  (cf. (2.5)). As long as the hierarchical scheme achieves this SINR, it is used; otherwise fully coordinated THP is chosen. Additionally, “very bad” channels for which even full THP gives  $\text{minSINR} < \text{minSINR}_{\text{out}}$  may be excluded from transmission at all (e.g., via higher protocol layers) and an *outage* may be declared.

Via the choice of  $\text{minSINR}_{\text{thr}}$  and  $\text{minSINR}_{\text{out}}$  a trade-off between performance and backhaul traffic is enabled. When lowering  $\text{minSINR}_{\text{thr}}$  the hierarchical scheme is more often sufficient and the backhaul signaling is reduced. Since the SINR depends on the channel SNR, a trade-off between minimally required SNR (e.g., to guarantee  $\text{BER} \leq 10^{-4}$ ) and backhaul traffic  $E\{\beta\}$  is possible, see Fig. 2.8.

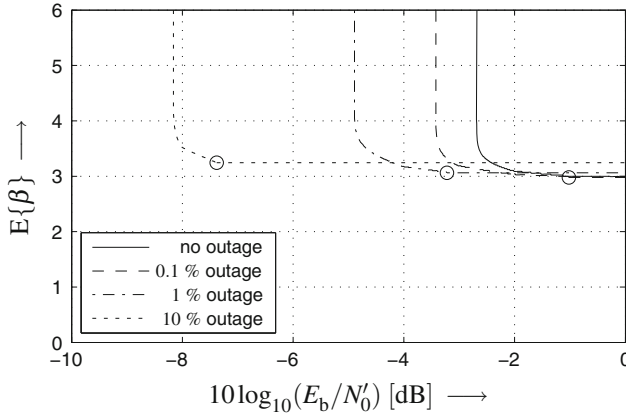


**Fig. 2.8** Trade-off between minimum required SNR and average backhaul traffic to obtain a BER of  $10^{-4}$ . 16QAM constellation; APC  $P_B = 1.5 \sigma_a^2$ . Curves go over into a horizontal branch when  $\min\text{SINR}_{\text{thr}} < \min\text{SINR}_{\text{out}}$  (marked by circles)

When setting  $\min\text{SINR}_{\text{thr}} = \infty$ , the selection is disabled and conventional THP (with APC) is chosen leading to  $\beta = 6$  but the lowest required SNR. If  $\min\text{SINR}_{\text{thr}}$  is lowered, the hierarchical scheme is selected more often and  $E\{\beta\}$  decreases but the required SNR increases slightly. Only if  $\min\text{SINR}_{\text{thr}}$  is very low, the hierarchical scheme is almost always active and  $E\{\beta\} \rightarrow 3$ . Allowing outage (0.1, 1, and 10 % in Fig. 2.8), the required SNR can significantly be lowered as the worst-case channels are eliminated. All curves go over into a horizontal branch when  $\min\text{SINR}_{\text{thr}} < \min\text{SINR}_{\text{out}}$ . For more details see [12].

### 2.3.4 Quantization of Precoded Symbols

The schemes discussed so far need to communicate *complex-valued* symbols via the backhaul. In practice, a quantization of these symbols is indispensable. Hence, another degree of freedom—the tradeoff between quantization error/performance and the required data rate (number of bits per symbol)—is enabled.

In this context, precoding based on integer forcing (cf. Sect. 2.2), specifically the *reverse compute-and-forward (RCoF) scheme* in [25] is of special interest. Since precoding is purely done over the finite field, only a few bits are required to communicate such symbols. However, in RCoF further joint preequalization via  $\mathbf{W}''$  (cf. Fig. 2.4 last row) or via a lower triangular  $\mathbf{F}$  (cf. Sect. 2.3.2) is not possible. Hence, performance is degraded for lowering the backhaul traffic.

## 2.4 Precoding for Finite-Field Channels

In Sect. 2.1.3 we discussed the usefulness of dualities and analogies in communications and pointed out that PC and NC are related in some sense. We now substantiate this point of view by presenting two precoding approaches for finite-field matrix channels, which can be seen as counterparts of conventional approaches for real (or complex) valued channels: *differential linear network coding (DLNC)* related to differential encoding, and *selection precoding (SP)* as a counterpart to vector precoding. All definitions of Sect. 2.1.2 apply here again.

### 2.4.1 Differential Linear Network Coding

The common approach for communicating over the MAMC is the usage of *lifted rank metric codes* [30, 39], which results in a rate loss  $L_{\text{lft}} \stackrel{\text{def}}{=} n/l$ , where  $l$  is the packet length and  $n$  is the number of simultaneously transmitted packets (cf. Sect. 2.1.2). This loss arises due to the lifting operation, i.e., transmitting the identity matrix at the beginning of each generation, which can be seen as pilot symbols for channel sounding. In the following, we present an approach that overcomes this drawback.

In case of *differential phase-shift keying (DPSK)* [36], information is transmitted in the phase transition between two consecutive transmit symbols, rather than in the absolute phase. Thus, any constant phase offset caused by the channel (and not known to the receiver) can be eliminated, at the cost of a (slightly) degraded performance compared to coherent transmission. We adopt this idea to the RLNC scenario, which is described by the MAMC (cf. Sect. 2.1.2, working over  $\mathbb{F}_q$ )

$$Y = AX + E. \quad (2.6)$$

Information is not represented directly in the matrix  $X$ , but in the transition between two consecutive transmit matrices. Such an idea was also present in the field of differential space-time codes [26, 27, 31, 43]. As a consequence, a *constant* multiplicative distortion  $A$  is irrelevant to the receiver. To obtain a constant network channel matrix, we force the intermediate nodes to keep their linear coding coefficients constant during the transmission. However, changes in the network channel matrix can occur when intermediate nodes leave or join the network, e.g., due to system failures, low battery, or system reboots.

If nodes leave or join the network between generations, the change of the network channel matrix can be expressed as

$$A_i = A_{i-1} + \Delta A_i, \quad (2.7)$$

where  $A_i$  denotes the network channel matrix in generation  $i$  and  $\Delta A_i$  the *channel deviation*. In [8], it has been shown that the rank of the channel deviation is upper



bounded by the sum of the *node weights* of the leaving/joining nodes. The node weight of a node  $v$  is defined as  $w(v) \stackrel{\text{def}}{=} \min\{n, \text{In}\{v\}, \text{Out}\{v\}\}$ , where  $\text{In}\{v\}$  and  $\text{Out}\{v\}$  denote the numbers of  $v$ 's incoming and outgoing edges, respectively. We call networks with a very small probability of leaving/joining nodes as *slowly-varying networks*.

For brevity let us restrict to square matrices, i.e.,  $n = N = L$ ; the generalization to non-square matrices can be found in [8, 10]. For differential modulation, we assume to have a sequence of full rank source words  $S_i$ . The DLNC transmit symbol in generation  $i$  is generated as

$$X_i = X_{i-1} \cdot S_i, \quad (2.8)$$

where  $X_0 \stackrel{\text{def}}{=} I_n$  ( $I_n$ : identity matrix of dimension  $n$ ) is the initialization word.

Differential demodulation at the destination node is done by calculating the product  $Y_{i-1}^+ \cdot Y_i$ , where  $Y_{i-1}^+$  is the pseudoinverse of the previously received matrix. This results in the demodulated symbol  $\tilde{S}_i$  [8]

$$\tilde{S}_i \stackrel{\text{def}}{=} Y_{i-1}^+ \cdot Y_i = S_i + \tilde{E}_i, \quad (2.9)$$

where  $\tilde{E}_i$  is the *effective error matrix*. Thus, the application of differential modulation and demodulation transforms the MAMC into an AMC with additive error  $\tilde{E}_i$ , as visualized in Fig. 2.9. The effective error comprises the effects of the differential demodulation process and of the slowly varying network. The former causes the additive error to have (approximately) doubled rank compared to the underlying channel, cf. noncoherent demodulation of DPSK where the error variance is doubled. The latter causes a rarely occurring impulsive rank error, which is equal to the rank of  $\Delta A$ .

When applying the differential approach, we are restricted to full-rank transmit matrices  $S_i$ , and thus, suffer a rate loss, well approximated by  $L_{\text{dlnc}} = 1/q$ , cf. [30]. This loss is negligible as long as  $q$  is large, which is a prerequisite in RLNC. More challenging are the circumstances that the additive errors occur in pairs, and that the scheme is sensitive to network topology variations. Due to the resulting effective error structure in DLNC—the doubled additive error, plus the rarely occurring impulsive

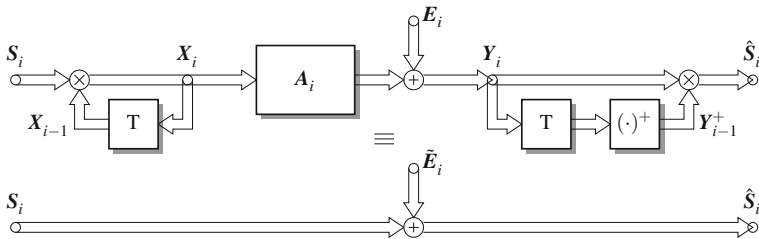


**Fig. 2.9** Block diagram of a DLNC scheme, converting the MAMC into an AMC. The “T”-block depicts a unit delay element

error peaks caused by leaving/joining nodes—the commonly applied rank-metric Gabidulin block codes [22] are no longer the best choice. Instead of these block codes, convolutional-type codes are preferable. In [8], it was shown that in particular *partial unit memory* Gabidulin codes [48] match to the present situation. Using them, higher reliabilities and/or higher rates are possible via DLNC compared to the lifting approach in slowly varying network coding applications.

### 2.4.2 Selection Precoding

In Sect. 2.2 the concept of modulo-type precoding for the MIMO broadcast channel was explained. The main idea in such schemes—THP and its generalization—is that each data symbol is represented by multiple, modulo congruent signal points; from this set the most suited one is selected for transmission. In doing so, the channel may not only be equalized but, additionally, desired properties of the transmit signal can be achieved, i.e., some kind of signal shaping is performed [19]. This principle can be transferred to finite-field channels, leading to a scheme denoted as *selection precoding (SP)* [2].

A prerequisite is the definition of modulo-congruent signal points in finite fields  $\mathbb{F}_{2^m}$ . This can be done in terms of cosets and the respective *coset decomposition*. Given an additive subgroup  $\mathbb{G}_{2^\mu}$  in  $\mathbb{F}_{2^m}$ ,  $\mu < m$ , the respective cosets are defined as

$$\mathcal{C}^{(\zeta)} \stackrel{\text{def}}{=} \{e_\zeta + a \mid a \in \mathbb{G}_{2^\mu}\}, \quad e_\zeta \in \mathbb{F}_{2^m}. \quad (2.10)$$

The *coset leaders*  $e_\zeta$  are then used as data-carrying symbols; all elements within the coset are modulo congruent and represent the same information. Given the data symbols  $e_\zeta$  any element from  $\mathbb{G}_{2^\mu}$  can be added without change of information. Conversely, given any element  $x \in \mathbb{F}_{2^m}$  a *finite field modulo operation* can be defined such that the coset leader  $e_\zeta$  of the corresponding coset, i.e.,  $x \in \mathcal{C}^{(\zeta)}$ , is returned.

The structure of the selection precoding scheme is depicted in Fig. 2.10. For brevity, we restrict ourselves to the MMC and square network channel matrices  $\mathbf{A}$ ; the generalization is easily possible. The elements of the source matrix  $\mathbf{S}$  are drawn from the set of coset leaders  $e_\zeta$ . A precoding matrix  $\mathbf{U}$ , whose elements are drawn from the subgroup  $\mathbb{G}_{2^\mu}$ , is added to obtain the *effective data matrix*  $\mathbf{V} \stackrel{\text{def}}{=} \mathbf{S} + \mathbf{U}$ .

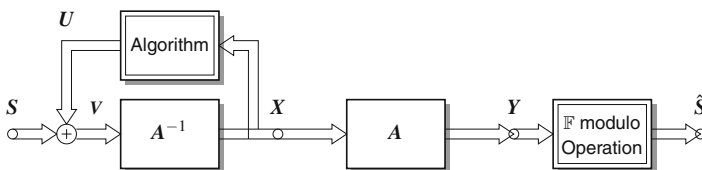


**Fig. 2.10** Selection precoding for the multiplicative matrix channel

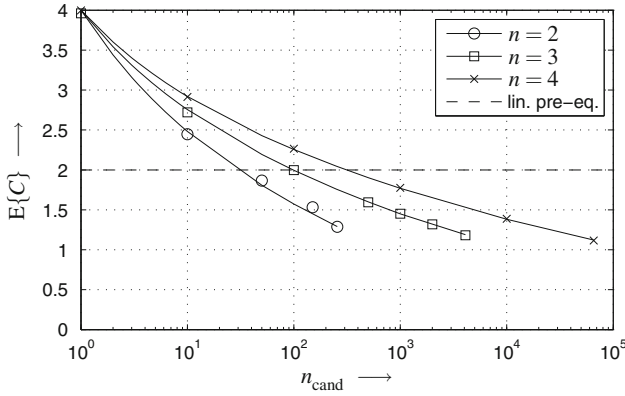


**Fig. 2.11** Average cost per symbol over the number of tested candidates for the selection precoding scheme with  $n = 2, 3$ , and  $4$ .  $\mathbb{F}_{2^8}$  and  $\mathbb{G}_{16}$ , i.e.,  $m = 8$  and  $\mu = 4$

This matrix is precoded via<sup>4</sup>  $\mathbf{A}^{-1}$ , thus, the SP transmit matrix, which is injected into the network, is given as  $\mathbf{X} = \mathbf{A}^{-1}\mathbf{V}$ . Assuming error-free transmission, the receive matrix is  $\mathbf{Y} = \mathbf{V}$ . After an (element-wise) finite-field modulo operation (recovery of the coset leader), the source symbols are perfectly recovered, i.e.,  $\hat{\mathbf{S}} = \mathbf{S}$ .

In [2], we have shown how to adapt the optimization to the current situation, i.e., how to find the optimum precoding matrix  $\mathbf{U}_{\text{opt}}$ . To this end, an optimization criterion has to be defined. This can be done in terms of a *cost function*  $C(\mathbf{X})$ , which assigns a non-negative, real-valued cost to each finite-field matrix  $\mathbf{X} \in \mathbb{F}_{2^m}^{n \times n}$ . In [2], two examples are given, namely the number of ones (i.e., the Hamming weight) and the number of signal changes in the binary vector representation of the  $\mathbb{F}_{2^m}$  elements.<sup>5</sup>

Then, the optimization problem reads

$$\mathbf{U}_{\text{opt}} = \underset{\mathbf{U} \in \mathbb{G}_{2^\mu}^{n \times t}}{\text{argmin}} C(\mathbf{A}^{-1}(\mathbf{S} + \mathbf{U})) . \quad (2.11)$$

This search may be accomplished in a random fashion, i.e., by randomly generating  $n_{\text{cand}}$  candidate precoding matrices  $\mathbf{U}$ , and selecting the one, which leads to the lowest transmit cost. Via  $n_{\text{cand}}$  a performance/complexity trade-off is enabled.

In Fig. 2.11 the average cost  $E\{C\}$  per symbol is plotted over the number  $n_{\text{cand}}$  of tested candidates per transmission block for  $n = 2, 3$ , and  $4$ . The coset decomposition of  $\mathbb{F}_{2^8}$  is generated with respect to  $\mathbb{G}_{16}$ . The solid lines represent the analytically derived average cost per symbol, cf. [2]. From the simulations results, which perfectly

<sup>4</sup>Again, we assume the network channel matrix to be a full rank matrix. However, it is known from the conventional setting that non-linear schemes (e.g., THP) can even be used on singular channels where linear schemes fail. This stabilization due to the multiple representation of symbols and the degree of freedom to choose from them is an additional advantage of the present scheme.

<sup>5</sup>Both cost functions have the same distribution for the cost and, thus, lead to the same performance.

match with the analytic solution, we can conclude that employing selection precoding is able to achieve a lower average cost than the reference scheme (dashed lines) at the same rate.

**Acknowledgments** The work of Robert Fischer and Johannes Huber was supported by the German Research Foundation (DFG) under Grants FI 982/4-1, FI 982/4-2, FI 982/4-3, and HU 634/11-3, respectively.

## References

### Project-Related Publications

1. Abay Ü, Fischer RFH (2011) Comparison of generalized tomlinson-harashima precoding strategies for the broadcast channel. In: Proceedings of international ITG workshop on smart antennas (WSA), Aachen, Germany, Feb 2011
2. Cyran M, Fischer RFH, Huber JB (2014) Selection precoding for the finite-field multiplicative matrix channel. *IEEE Commun Lett* 18(2):360–363
3. Fischer RFH (2010) From gram-schmidt orthogonalization via sorting and quantization to lattice reduction. In: Proceedings of joint workshop on coding and communications (JWCC), Santo Stefano Belbo, Italy, Oct 2010
4. Fischer RFH (2011) Efficient Lattice-reduction-aided mmse decision-feedback equalization. In: Proceedings of international conference on acoustics, speech and signal processing (ICASSP), Prag, Czech Republic, May 2011
5. Fischer RFH (2012) Complexity-performance trade-off of algorithms for combined lattice reduction and QR decompositions. *Int J Electron Commun (AEÜ)* 66(11):871–879
6. Fischer RFH, Heinrichs S (2013) The network MIMO Downlink with per-antenna power constraint: linear preequalization vs. tomlinson-harashima precoding. In: Proceedings of international ITG workshop on smart antennas (WSA), Stuttgart, Germany, Mar 2013
7. Fischer RFH, Windpassinger C, Stierstorfer C, Siegl C, Schenk A, Abay Ü (2011) Lattice-reduction-aided MMSE equalization and the successive estimation of correlated data. *Int J Electron Commun (AEÜ)* 65(8):688–693
8. Puchinger S, Cyran M, Fischer RFH, Bossert M, Huber JB (2015) Error correction for differential linear network coding in slowly-varying networks. In: Proceedings of international ITG conference on systems, communications and coding (SCC), Hamburg, Germany, Feb 2015
9. Schotsch B, Cyran M, Huber JB, Fischer RFH, Vary P (2015) An upper bound on the outage probability of random linear network codes with known incidence matrices. In: Proceedings of international ITG conference on systems, communications and coding (SCC), Hamburg, Germany, Feb 2015
10. Seidl M, Cyran M, Fischer RFH, Huber JB (2013) A differential encoding approach to random linear network coding. In: Proceedings of international ITG Conference on systems, communications and coding (SCC), Munich, Germany, Jan 2013
11. Stern S, Fischer RFH (2015) Hierarchical precoding for the network MIMO downlink. In: Proceedings of international ITG conference on systems, communications and coding (SCC), Hamburg, Germany, Feb 2015
12. Stern S, Fischer RFH (2015) Selection of the coordination strategy in the network MIMO downlink. In: Proceedings of international ITG workshop on smart antennas (WSA), Ilmenau, Germany, Mar 2015
13. 3GPP (2002) Technical Specification Group Radio Access Network, RF System Scenarios, Technical Report TR 25.996 V3.3.0, 2002

## Additional Literature

14. 3GPP (2006) Technical Specification Group Radio Access Network, Physical Layer Aspects for Evolved Universal Terrestrial Radio Access (UTRA), Technical Report TR 25.814 V7.1.0, 2006
15. Ahlswede R, Cai N, Li SYR, Yeung RW (2000) Network information flow. *IEEE Trans Inf Theory* 46(4):1204–1216
16. Ancheta TC (1976) Syndrome-source-coding and its universal generalization. *IEEE Trans Inf Theory* 22(4):432–436
17. Caire G, Shamai S, Verdú S (2003) Lossless data compression with error correcting codes. In: *Proceedings of the international symposium on information theory 2003*, Yokohama, Japan, Jun/Jul 2003
18. Feng C, Silva D, Kschischang FR (2013) An algebraic approach to physical-layer network coding. *IEEE Trans Inf Theory* 59(11):7576–7596
19. Fischer RFH (2002) *Precoding and signal shaping for digital transmission*. Wiley, New York
20. Fischer RFH, Windpassinger C, Lampe A, Huber JB (2002) Space-time transmission using tomlinson-harashima precoding. In: *Proceedings of the international ITG conference on source and channel coding (SCC)*, Berlin, Germany, pp. 139–147, Jan 2002
21. Foschini G (1996) Layered space-time architecture for wireless communication in a fading environment when using multiple antennas. *Bell Laboratories Tech J* 41–59
22. Gabidulin EM (1985) Theory of codes with maximum rank distance. *Probl Inf Transm* 21(1):1–12
23. Golden G, Foschini G, Valenzuela R, Wolniansky P (1999) Detection algorithm and initial laboratory results using the V-BLAST space-time communication architecture. *Electron Lett* 14–15
24. Gupta A, Verdú S (2011) Operational duality between lossy compression and channel coding. *IEEE Trans Inf Theory* 57(6):3171–3179
25. Hong SN, Caire G (2013) Compute-and-forward strategies for cooperative distributed antenna systems. *IEEE Trans Inf Theory* 59(9):5227–5243
26. Hochwald BM, Sweldens W (2000) Differential unitary space-time modulation. *IEEE Trans Commun* 48(12):2041–2052
27. Hughes BL (2000) Differential space-time modulation. *IEEE Trans Inf Theory* 46(7):2567–2578
28. Jindal N, Vishwanath S, Goldsmith AJ (2004) On the duality of gaussian multiple-access and broadcast channels. *IEEE Trans Inf Theory* 50(5):768–783
29. Karakayali MK, Foschini GJ, Valenzuela RA (2006) Network coordination for spectrally efficient communication in cellular systems. *IEEE Wirel Commun* 13(4):56–61
30. Kötter R, Kschischang FR (2008) Coding for errors and erasures in random linear network coding. *IEEE Trans Inf Theory* 54(8):3579–3591
31. Lampe L, Schober R, Fischer RFH (2003) Coded differential space-time modulation for flat fading channels. *IEEE Trans Wireless Commun* 2(3):582–590
32. Lenstra A, Lenstra H, Lovász L (1982) Factoring polynomials with rational coefficients. *Mathematische Annalen* 515–534
33. Nazer B, Gastpar M (2011) Compute-and-forward: harnessing interference through structured codes. *IEEE Trans Inf Theory* 57(10):6463–6486
34. Ordentlich O, Erez E, Nazer B (2013) Successive integer-forcing and its sum-rate optimality. In: *Annual allerton conference on communication, control, and computing*, Allerton, USA, pp 282–292, Oct 2013
35. Peel CB, Hochwald BM, Swindlehurst AL (2005) A Vector-perturbation technique for near-capacity multiantenna multiuser communication-part i: channel inversion and regularization. *IEEE Trans Commun* 53(1):195–202
36. Proakis J, Salehi M (2008) *Digital communications*, 5th edn. McGraw-Hill
37. Sakzad A, Harshan J, Viterbo E (2013) Integer-forcing MIMO linear receivers based on lattice reduction. *IEEE Trans Wireless Commun* 12(10):4905–4915

38. Schubert M, Boche H (2002) A unifying theory for uplink and downlink multi-user beamforming. In: IEEE International zurich seminar (IZS), Zurich, Switzerland, Feb 2002
39. Silva D, Kschischang FR, Kötter R (2008) A rank-metric approach to error control in random linear network coding. *IEEE Trans Inf Theory* 54(9):3951–3967
40. Silva D, Kschischang FR, Kötter R (2010) Communication over finite-field matrix channels. *IEEE Trans Inf Theory* 56(3):1296–1305
41. Stierstorfer C, Fischer RFH (2006) Lattice-reduction-aided tomlinson-harashima precoding for point-to-multipoint transmission. *Int J Electron Commun (AEÜ)* 60(4):328–330
42. Stierstorfer C, Siegl C, Fischer RFH, Wild T, Hoek C (2010) Network MIMO downlink transmission. In: Proceedings of international OFDM workshop (InOWo), Hamburg, Germany, Sept 2010
43. Tarokh V, Jafarkhani H (2000) A differential detection scheme for transmit diversity. *IEEE J Sel Areas Commun* 18(7):1169–1174
44. Taherzadeh M, Mobasher A, Khandani AK (2007) LLI reduction achieves the receive diversity in MIMO decoding. *IEEE Trans Inf Theory* 53(12):4801–4805
45. Tölli A, Codreanu M, Juntti M (2008) Linear multiuser MIMO transceiver design with quality of service and per-antenna power constraints. *IEEE Trans Signal Process* 56(7):3049–3055
46. Viswanath P, Tse DNC (2003) Sum capacity of the vector gaussian broadcast channel and uplink-downlink duality. *IEEE Trans Inf Theory* 49(8):1912–1921
47. Vishwanath S, Jindal N, Goldsmith A (2003) Duality, achievable rates, and sum-rate capacity of gaussian MIMO broadcast channels. *IEEE Trans Inf Theory* 49(10):2658–2668
48. Wachter A, Sidorenko VR, Bossert M, Zyablov VV (2011) On (Partial) unit memory codes based on gabidulin codes. *Prob Inf Transm* 47(2):117–129
49. Weingarten H, Steinberg Y, Shamai S (2006) The capacity region of the Gaussian multiple-input multiple-output broadcast channel. *IEEE Trans Inf Theory* 52(9):3936–3964
50. Windpassinger C (2004) Detection and precoding for multiple input multiple output channels. Ph.D. Thesis, Friedrich-Alexander-Universität Erlangen-Nürnberg
51. Windpassinger C, Fischer RFH (2003) Low-complexity near-maximum-likelihood detection and precoding for MIMO systems using lattice reduction. In: IEEE information theory workshop, Paris, France, pp 345–348, Mar/Apr 2003
52. Windpassinger C, Fischer RFH, Huber JB (2004) Lattice-reduction-aided broadcast precoding. *IEEE Trans Commun* 52(12):2057–2060
53. Wübben D, Böhnke R, Kühn V, Kammeyer KD (2004) Near-maximum-likelihood detection of MIMO systems using MMSE-based lattice reduction. In: IEEE International conference on communications, Paris, France, pp 798–802, Jun 2004
54. Wübben D, Seethaler D, Jalden J, Matz G (2011) Lattice reduction. *IEEE Signal Process Mag* 28(3):70–91
55. Yao H, Wornell GW (2002) Lattice-reduction-aided detectors for MIMO communication systems. In: IEEE global telecommunications conference, Taipei, Taiwan, pp 424–428, Nov 2002
56. Yu W, Cioffi JM (2004) Sum capacity of Gaussian vector broadcast channels. *IEEE Trans Inf Theory* 50(9):1875–1892
57. Yu W, Lan T (2007) Transmitter optimization for the multi-antenna downlink with per-antenna power constraints. *IEEE Trans Signal Process* 55(6):2646–2660
58. Zamir R, Shamai S, Erez U (2002) Nested linear/lattice codes for structured multiterminal binning. *IEEE Trans Inf Theory* 48(6):1250–1276
59. Zhan J, Nazer B, Erez U, Gastpar M (2014) Integer-forcing linear receivers. *IEEE Trans Inf Theory* 60(12):7661–7685

Communications in Interference Limited Networks

Utschick, W. (Ed.)

2016, XI, 519 p. 177 illus., 100 illus. in color., Hardcover

ISBN: 978-3-319-22439-8